Organic & Biomolecular Chemistry

PAPER

View Article Online
View Journal | View Issue

Cite this: *Org. Biomol. Chem.*, 2017, **15**, 1190

Fluorescence enhancement of oligodeoxynucleotides modified with green fluorescent protein chromophore mimics upon triplex formation†

Takashi Kanamori, Akihiro Takamura, Nobuhiro Tago, Yoshiaki Masaki, Akihiro Ohkubo, Mitsuo Sekine* and Kohji Seio*

Received 14th June 2016,
Accepted 23rd December 2016

DOI: 10.1039/c6ob01278g

rsc.li/obc

Green fluorescent protein (GFP)-based molecular-rotor chromophores were attached to the 5-positions of deoxyuridines, and subsequently, incorporated into the middle positions of oligodeoxynucleotides. These oligonucleotides were designed to form triplex DNA in order to encapsulate the GFP chromophores, mimicking GFP structures. Upon triplex formation, the embedded GFP chromophores exhibited fluorescence enhancement, suggesting the potential application of these fluorescent probes for the detection of nucleic acids.

Introduction

Fluorescent oligonucleotides have been extensively used as fluorescent probes for the detection and structural determination of biologically functional nucleic acids.[1] One of the essential properties of the fluorescent probes is that they emit fluorescence only when they bind to their target molecules or form specific structures. To further explore the potential of these probes, fluorescent nucleotides having switchable emissive properties must be developed.

The emissions of fluorescent nucleosides can be controlled by various mechanisms. For example, the popular fluorescent nucleoside 2-aminopurine riboside[2] undergoes fluorescence changes in response to microhydration[3] and stacking with nearby nucleobases.[4] Recently, a group of fluorescent molecules known as "molecular rotors" has widely been investigated.[5]

Molecular rotor-type fluorescent dyes contain a rotatable chemical bond which is crucial for their fluorescence properties. Under the conditions in which the bond can rotate, the dyes emit only very weak fluorescence because the dyes in their excited states lose energy through nonradiative pathways which involve the internal rotation around the bond. However, when the internal rotation of the bond is restricted, the radiative relaxation pathways become dominant, and the dyes emit strong fluorescence. Thus, oligonucleotides incorporating molecular rotor-type fluorescent residues can be used as fluorescent oligonucleotide probes which emit stronger fluorescence when they form complexes with target nucleic acids or proteins in which the conformation of the molecular rotor is restricted.[5]

Interestingly, the naturally occurring green fluorescent protein (GFP)[6] contains a molecular rotor-type fluorophore having a (4-hydroxybenzylidene)imidazolin-3-one skeleton.[7] In such proteins, this residue is forced to become planar due to its interaction with the surrounding amino acid residues, and thus, emits strong fluorescence.[8] Therefore, if (4-hydroxybenzylidene)imidazolin-3-one or its derivatives were introduced into the appropriate positions of oligonucleotides, such oligonucleotides would become useful molecular rotor-type fluorescent probes. Indeed, Hocek and co-workers have reported deoxycytidine incorporating a (3,5-difluoro-4-hydroxybenzylidene)-2-methylimidazolin-3-one (FBI) residue as a molecular rotor,[5c] which exhibits fluorescence enhancement by 2.0–3.5 times upon its interaction with DNA binding proteins. In addition, Stafforst and Diederichsen reported peptide nucleic acids (PNAs) incorporating a (4-hydroxybenzylidene)-2-methylimidazolin-3-one (HBI) residue and their fluorescence enhancement by *ca.* 2.2 times upon the formation of PNA–DNA duplexes.[9] Thus, the incorporation of FBI and HBI residues affords oligonucleotides which emit fluorescence in various structural contexts such as DNA–protein interactions[5c,d] and duplex formation. However, the increase of the fluorescence intensity upon binding to the targets is at best 2 to

Department of Life Science, Tokyo Institute of Technology, 4259 Nagatsuta-Cho, Midori-ku, Yokohama 226-8501, Japan. E-mail: msekine@bio.titech.ac.jp, kseio@bio.titech.ac.jp

†Electronic supplementary information (ESI) available: Experimental procedures, ^{1}H, and ^{13}C NMR charts; ESI-TOF mass data for the compounds and MALDI-TOF mass data and HPLC charts for the oligonucleotides. See DOI: 10.1039/c6ob01278g

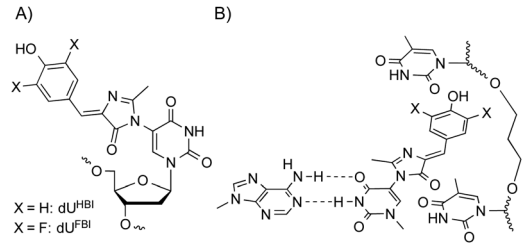

Fig. 1 (A) Structures of dU^{HBI} and dU^{FBI} residues, and (B) the illustration of their triplex-induced fluorescence configurations.

4 times greater. A higher fluorescence increase is preferable for further applications.

To obtain higher fluorescence on/off rates, we tried to combine the HBI-type chromophore with the previously reported fluorescence system[5e] using a DNA triplex (see below). Here, we designed deoxyuridine derivatives having an HBI or FBI residue directly attached to the 5-position of the uracil ring (Fig. 1). We prepared DNA duplexes incorporating these uridine derivatives, and studied their fluorescence enhancement in the presence of triplex-forming oligodeoxynucleotides (TFOs). We have previously reported the TFO-induced fluorescence of DNA duplexes incorporating 5-(3-methylbenzofuran-2-yl)deoxyuridine (dU^{MBF}),[5e] and the application of the TFO-induced fluorescence to a model experiment for the detection of micro RNAs. In this system, the single stranded target DNA strand reverse-transcribed from the microRNA is captured by the single stranded ODN containing dU^{MBF} forming Watson–Crick base pairs, and the fluorescence of dU^{MBF} was enhanced by the formation of the DNA triplex, using the TFO-incorporating C3 residue.

In this triplex, the methylbenzofuran moiety protrudes into the major groove and is covered by the nucleobases around the abasic site in the TFO. The formation of the triplex enhanced fluorescence by 16 times in comparison with that observed in the absence of the TFO. Therefore, if the oligonucleotides modified with HBI and FBI show similar triplex-induced large fluorescence enhancement as shown in Fig. 1, they might be utilized for the detection of biologically important nucleic acids in combination with dU^{MBF}.

Results and discussion

Synthesis of nucleoside phosphoramidites

First, the protected (4-hydroxybenzylidene)-2-methylimidazolinone (**3a**) was prepared (Scheme 1). The hydroxy group of 4-hydroxybenzaldehyde (**1a**) was protected using a pivaloyloxymethyl (POM) group to give **2a** in 66% yield. Under previously reported conditions,[7a,10] compound **2a** was condensed with *N*-acetylglycine to give the oxazoline derivative **3a** in 33% yield. Similarly, the protected 3,5-difluoro-4-hydroxybenzylidene derivative **3b** was synthesized from 3,5-difluoro-4-hydroxybenzaldehyde (**1b**). 3′,5′-Di-*O*-acetyl-5-nitro-deoxyuridine (**4**)[11] was separately hydrogenolyzed to the 5-amino

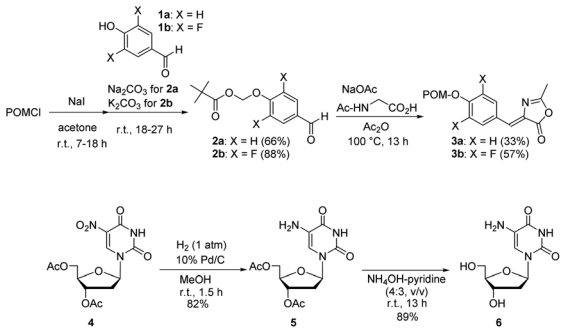

Scheme 1 Synthesis of intermediates: (4-hydroxybenzylidene)-2-methylimidazolinone derivative (**3a**), (3,5-difluoro-4-hydroxybenzylidene)-2-methylimidazolinone derivative (**3b**), and 5-aminodeoxyuridine (**6**).

derivative **5** in 82% yield in the presence of 10% Pd/C. Subsequently, the acetyl groups were removed by treatment with aqueous ammonia in pyridine to give 5-amino-2′-deoxyuridine (**6**)[12] in 89% yield. By the use of **3a**, **3b**, and **6**, dU^{HBI} (**8a**) and dU^{FBI} (**8b**) were synthesized as shown in Scheme 2.

Using previously reported conditions,[10] compound **3a** or **3b** was condensed with **6** in pyridine at 60 to 90 °C for **3a** or 40 °C for **3b** to give POM-protected dU^{HBI} (**7a**) in 42% and dU^{FBI} (**7b**) in 55%, respectively. The subsequent deprotection of the POM groups of **7a** and **7b** gave the desired **8a** and **8b**, respectively.

In addition, for oligonucleotide synthesis, **7a** and **7b** were converted to the phosphoramidites **10a** and **10b** *via* the 5′-DMTr derivatives **9a** and **9b**, respectively. The phosphoramidites were directly used for oligonucleotide synthesis after usual work-up.

Fluorescence properties of nucleosides

The fluorescence properties of **8a** and **8b** were studied (Fig. 2). Compound **8a** shows a maximum absorbance in both methanol and glycerol–methanol solutions at around 376 nm, which

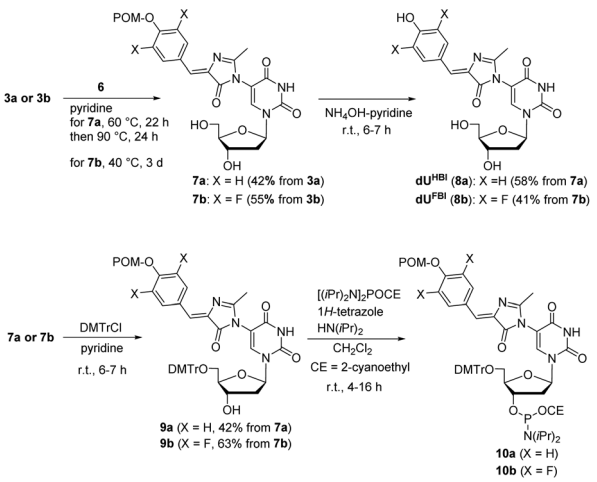

Scheme 2 HBI- and FBI-modified deoxyuridines (**8a** and **8b**, respectively), and their phosphoramidites.

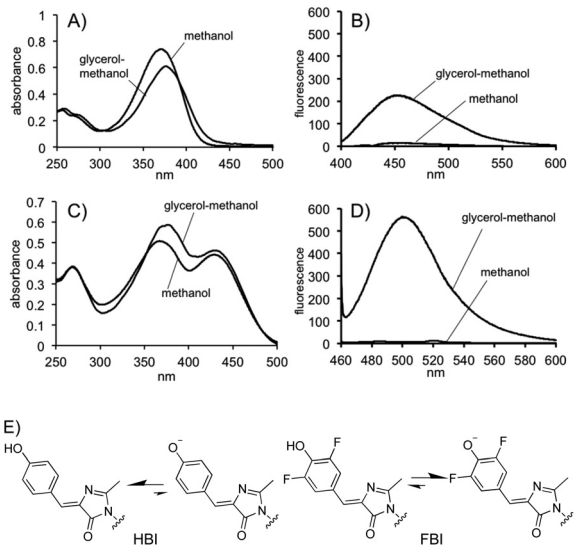

Fig. 2 Photophysical properties of **8a** and **8b**. The absorption spectra of (A) **8a** and (C) **8b** (30 μM) in glycerol–methanol (95 : 5, v/v) or methanol solution, and the fluorescence spectra of (B) **8a** (100 μM, λ_{ex} 380 nm) and (D) **8b** (1 μM, λ_{ex} 430 nm) in the glycerol–methanol or methanol solution. (E) Structures of the protonated and de-protonated forms of HBI and FBI residues.

is close to that of HBI (Fig. 2A).[13] It also shows a smaller absorbance at around 260 nm which is close to that of uracil. Upon irradiation at 380 nm, the glycerol–methanol solution of **8a** emits fluorescence at around 453 nm, whereas the methanol solution emits only very weak fluorescence (Fig. 2B). It had been reported that HBI derivatives emitted strong fluorescence signals in viscous glycerol.[9] Thus, these results suggest that the molecular-rotor like properties of HBI are retained even after its placement on the uracil ring.

The photophysical properties of **8b** were similarly studied. As shown in Fig. 2C, compound **8b** exhibits a maximum absorption at around 377 nm, which is very close to that of **8a**, and a second absorption at around 430 nm in both solvents. The absorption at a longer wavelength is expected to be that of the deprotonated form of **8b** having a difluorophenolate anion, because the wavelength is very close to the maximum wavelength of **8a** or **8b** in the presence of sodium methoxide (see Fig. S5†). Thus, in glycerol–methanol solution, compound **8b** is expected to be in an equilibrium between the deprotonated and protonated forms of the difluorophenol moiety. Upon excitation at 430 nm, the glycerol–methanol solution of **8b** shows a maximum fluorescence at 500 nm, a longer wavelength in comparison with that of **8a** (Fig. 2D). It should be noted that the above fluorescence spectra were measured using a 100 μM solution of **8a** and 1 μM solution of **8b**. Thus, a comparison of the observed fluorescence intensity of the 100 μM solution of **8a**, which was about 200, and that of the 1 μM solution of **8b**, which was about 550, suggests that **8b** emits much stronger fluorescence. In addition, because of the lower pK_a of the phenolic proton, **8b** emits a longer wavelength than **8a** does, which is attributed to the deprotonated form of the difluorophenol ring (Fig. 2E).

Thermal stabilities of DNA triplexes incorporating HBI and FBI residues

Next, to study the fluorescence properties of ODNs and DNA triplexes incorporating dU^{HBI} and dU^{FBI}, ODNs were synthesized on an automated DNA/RNA synthesizer using phosphoramidites **10a** and **10b**. The sequences of the synthesized and purchased oligonucleotides are shown in Fig. 3. **ODN-1** is an oligodeoxynucleotide containing only canonical deoxynucleotides. **ODN-2-H** and **ODN-2-F** incorporate dU^{HBI} and dU^{FBI} at position Y, respectively, each of which forms an antiparallel duplex with **ODN-1**. We also synthesized **TFO-C3** and **TFO-A**, which form parallel triplexes with duplexes **ODN-2-H**/**ODN-1** or **ODN-2-F**/**ODN-1**. **TFO-C3** has a propylene linker, C3, at the position opposite to Y. In the TFO, 2-aminopyridine (Py) residues, with pK_a = 5.9, were introduced instead of cytosine so that the TFOs would bind to the duplexes even under neutral pH conditions.[14]

Using the ODNs, we first studied triplex formation. The UV melting experiments of a solution of **ODN-1**, **ODN-2-H**, and **TFO-C3** (2 μM each) showed two transitions near 35 and 62 °C (Fig. S6A†). The transition at a lower temperature corresponds to the melting of the **ODN-1**/**ODN-2-H**/**TFO-C3** triplex to the **ODN-1**/**ODN-2-H** duplex and **TFO-C3**, and the other transition corresponds to the further melting of the **ODN-2-H**/**ODN-1** duplex into single strands. In the case of the triplex containing **TFO-A**, the same experiment gave the T_m of 41 °C (Fig. S6C†). By carrying out similar experiments, we determined the melting temperatures of the triplex **ODN-1**/**ODN-2-F**/**TFO-C3** and **ODN-1**/**ODN-2-F**/**TFO-A** as 34 °C and 39 °C, respectively (Fig. S6B and S6D†). The higher T_ms of the triplexes containing dA in comparison with those containing the C3 linker are probably because the backbone conformation of **TFO-A** is less flexible than that of **TFO-C3** owing to the presence of a cyclic structure in the deoxyribose residue.

Fluorescence properties of DNA triplexes incorporating HBI and FBI residues

Next, we studied the fluorescence properties of **ODN-2-H** and **ODN-2-F** in their single-strand states, as duplexes with **ODN-1**, and as triplexes. As shown in Fig. 4A, **ODN-2-H** emits only weak fluorescence in the single-strand and duplexed states,

ODN-1: 3'-d(GTTCTTTTTTCTATCTTTTTTTG)-5'
ODN-2-Y: 5'-d(CAAGAAAAAAGAYAGAAAAAAAC)-3'
ODN-2-H: Y = U^{HBI}; **ODN-2-F**: Y = U^{FBI}
TFO-Z: 5'-d(TTP$_y$TTTTTTP$_y$TZTP$_y$TTTTTTT)-3'
TFO-C3: Z = C3; **TFO-A**: Z = A

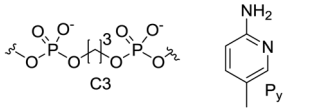

Fig. 3 Sequences of ODNs and TFO.

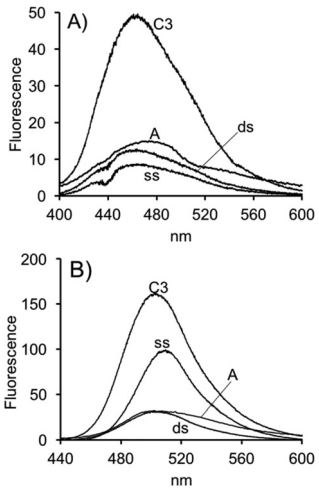

Fig. 4 Fluorescence spectra of (A) **ODN-2-H** and (B) **ODN-2-F** in their single-strand states (ss), as duplexes with **ODN-1** (ds), as triplexes **ODN-1**/**ODN-2-Y**/**TFO-C3** (C3), and as triplexes **ODN-1**/**ODN-2-Y**/**TFO-A** (A). Conditions: 2 μM oligonucleotides, 10 mM cacodylate buffer (pH 7.0), 10 mM $MgCl_2$, 500 mM NaCl.

probably because the HBI residue can freely rotate. However, upon the addition of **TFO-C3** to form the **ODN-1**/**ODN-2-H**/**TFO-C3** triplex, the fluorescence intensity at 465 nm increases by *ca.* 5.8 times. This result suggests that the molecular rotor-like properties of the HBI residue can be controlled by DNA triplex formation, as expected. The emission observed at 465 nm suggested that the HBI residue retained its protonated form in the single stranded, duplex, and triplex states. It is difficult to deprotonate the phenolic proton of HBI while retaining the triplex structure because it requires raising the pH of the solution to 8. Under such conditions, the Py residues are also deprotonated and the triplex is destabilized.

When the TFO is changed to **TFO-A**, the fluorescence intensity of the triplex decreased to levels comparable to those of the duplex. This result suggested that the large fluorescence enhancement of the DNA triplex incorporating HBI required TFO incorporating the abasic C3 site. Probably, the HBI residue is inserted into the space formed by the C3 linker and the upper and lower base as shown in Fig. 1. It should be noted that some molecular-rotor fluorophores such as SYBR green interact with the minor groove of the DNA duplex.[15] The observation that the HBI and FBI residues in the duplexes did not emit fluorescence suggested that the mechanisms of the fluorescence enhancement of dU^{HBI} and dU^{FBI} are different from that of these fluorophores.

In the case of **ODN-2-F** shown in Fig. 4B, the fluorescence unexpectedly decreases upon duplex formation. However, the fluorescence intensity at 502 nm of the triplex composed of **ODN-1**/**ODN-2-F**/**TFO-C3** is *ca.* 1.8 times higher than that of the single-strand state of **ODN-2-F**. The fluorescence intensity is much higher than that of the **ODN-1**/**ODN-2-H**/**TFO-C3** triplex. As a result, the fluorescence intensity of **ODN-2-F** in the triplex state is only *ca.* 1.8 times higher than that of the single strand, whereas the fluorescence of the **ODN-1**/**ODN-2-H**/**TFO-C3** triplex is *ca.* 5.8 times higher than that of single-strand **ODN-2-H**. The emission observed at 502 nm suggested that the FBI residue was in the deprotonated form in the single stranded, duplex, and triplex states. This observation is reasonable because the pK_a of the phenolic proton of FBI is *ca.* 5.5,[7a] which is much lower than the pH 7 solution conditions used in these experiments.

Conclusions

In this paper, we synthesized the new switchable fluorescent nucleosides, dU^{HBI} and dU^{FBI}, and oligonucleotides incorporating them as fluorophores, to mimic those of GFPs. We demonstrated their switchable fluorescence in response to DNA triplex formation. The results reported in this paper are the first examples of the fluorescence enhancement of HBI or FBI residues in combination with DNA triplex formation. The particular usefulness of the triplex system is demonstrated by the enhancement of the fluorescence of **ODN-2-H** by 5.8 times, which is greater than the previously reported oligonucleotide analogs modified with HBI.[5e,9]

Because DNA triplexes have been widely used in the development of the DNA nanostructures/nanomachines[16] and DNA biosensors,[5e,17] the triplex-induced fluorescence of dU^{HBI} and dU^{FBI} could also be applied to such nucleic acid technologies. For example, by using two ODN probes incorporating dU^{FBI} or the previously reported dU^{MBF},[5e] each of which is complementary to a different target nucleic acid, and appropriately designed TFOs, we can develop a detection system which can quantify two different target nucleic acids in a single test tube by monitoring the fluorescence at different wavelengths (dU^{FBI} at 500 nm and dU^{MBF} at 428 nm). Moreover, by developing other fluorescent nucleosides that emit at various wavelengths, multiplex nucleic acid detection systems might be developed. We are now investigating derivatives of dU^{HBI} and dU^{FBI}, incorporating various substituents on the phenol rings or changing the positions of OH groups, to realize such multiplex detection systems. Our results will be reported in due course.

Experimental

Materials

Reagents and dry solvents used for the synthesis of modified nucleosides and their phosphoramidite units were purchased from commercial sources. The dry solvents were stored over molecular sieves 4A. Reagents for DNA synthesis and unmodified DNA phosphoramidite units (dA, T, dG, dC) and CPG-columns were purchased from Glen Research. Sep-Pak C18 cartridges for DNA purification were purchased from Waters. Unmodified oligodeoxynucleotides were purchased from Sigma-Aldrich. ^1H and ^{13}C NMR spectra were obtained at 500 and 126 MHz, respectively. The chemical shifts were measured from DMSO in DMSO-d_6 (2.49 ppm) for ^1H NMR, 39.52 ppm

for ^{13}C NMR and $CHCl_3$ in $CDCl_3$ (7.26 ppm) for ^{1}H NMR, 77.16 ppm for ^{13}C NMR.

(4-Formylphenoxy)methyl pivalate (2a). Sodium iodide (4.05 g, 27.0 mmol) and chloromethyl pivalate (4.07 g, 27.0 mmol) were dissolved in dry acetone (50 mL) and stirred at room temperature under an argon atmosphere. After 7 h, sodium carbonate (2.86 g, 27.0 mmol) and 4-hydroxybenzaldehyde (**1a**) (3.00 g, 24.6 mmol) were added. The mixture was stirred for 19 h. After the completion of the reaction, diethyl ether was added and the precipitates were removed by filtration. The filtrate was evaporated and purified by C-200 silica gel chromatography with *n*-hexane–ethyl acetate (96 : 4, v/v) to give compound **2a** (3.84 g, 66%); ^{1}H NMR (500 MHz, chloroform-*d*) δ 9.93 (s, 1H), 7.87 (d, J = 9.0 Hz, 2H), 7.16 (d, J = 9.0 Hz, 2H), 5.84 (s, 2H), 1.20 (s, 9H); ^{13}C NMR (126 MHz, chloroform-*d*) δ 191.0, 177.3, 161.8, 132.1, 131.6, 116.3, 84.8, 39.2, 27.1. ESI-MS calcd for $C_{13}H_{16}NNaO_4^+$ $[M + Na]^+$ 259.0941; found 259.0934.

(*Z*)-[4-((2-Methyl-5-oxo-oxazolin-4-ylidene)methyl)phenyl]oxymethyl pivalate (3a). Compound **2a** (3.77 g, 16.0 mmol), *N*-acetylglycine (1.87 g, 16.0 mmol) and sodium acetate (1.31 g, 16.0 mmol) were dissolved in acetic anhydride (16 mL) and stirred at 100 °C for 13 h. The reaction mixture was diluted with ethyl acetate (400 mL) and washed with water. The organic layer was collected, evaporated and dried over Na_2SO_4. The crude product was purified by C-200 silica gel chromatography with *n*-hexane–ethyl acetate (85 : 15, v/v). Furthermore, the crude compound was dissolved in *n*-hexane–ethyl acetate (90 : 10, v/v, 30 mL) at 50 °C and cooled to room temperature. The precipitates were filtered to give compound **3a** (1.70 g, 33%); ^{1}H NMR (500 MHz, chloroform-*d*) δ 8.07 (d, J = 8.7 Hz, 2H), 7.12–7.07 (m, 3H), 5.82 (s, 2H), 2.39 (s, 3H), 1.21 (s, 9H). ^{13}C NMR (126 MHz, chloroform-*d*) δ 177.4, 168.1, 165.7, 159.2, 134.3, 131.4, 131.0, 128.0, 116.4, 85.0, 39.1, 27.1, 15.8. ESI-MS calcd for $C_{17}H_{19}NaO_5^+$ $[M + Na]^+$ 340.1155; found 340.1152.

3′,5′-Di-*O*-acetyl-5-amino-2′-deoxyuridine (5). To a solution of compound **4** [11] (1.60 g, 4.48 mmol) in methanol (800 mL), was added 10% Pd–C (224 mg) under an argon atmosphere. Then the argon was replaced with H_2 and the reaction mixture was stirred vigorously for 1.5 h at room temperature. Then, Pd–C was filtered using Celite and the filtrate was evaporated and purified by C-200 silica gel chromatography with dichloromethane–methanol (97 : 3, v/v) to give compound **5** (1.2 g, 82%); ^{1}H NMR (500 MHz, chloroform-*d*) δ 9.20 (s, 1H), 6.90 (s, 1H), 6.37 (dd, J = 8.6, 5.6 Hz, 1H), 5.20 (m, 1H), 4.46–4.29 (m, 2H), 4.29–4.13 (m, 1H), 3.48 (m, 2H), 2.44 (m, 1H), 2.19–2.12 (m, 7H); ^{13}C NMR (126 MHz, chloroform-*d*) δ 170.6, 160.5, 149.0, 122.9, 116.2, 84.9, 84.9, 82.1, 74.2, 74.2, 64.0, 37.1, 21.1. ESI-MS calcd for $C_{13}H_{17}N_3NaO_7^+$ $[M + Na]^+$ 350.0959; found 350.0961.

5-Amino-2′-deoxyuridine (6). To a solution of compound **5** (5.84 g, 17.8 mmol) in pyridine (60 mL) was added 28% NH_4OH (80 mL). The reaction mixture was stirred for 13 h at room temperature. Then, it was concentrated and the crude product was purified by C-200 silica gel chromatography with dichloromethane–methanol (85 : 5, v/v). The fractions containing the target compound were concentrated. The residue was precipitated by the addition of methanol and filtered to give compound **6** [12] (3.85 g, 89%); ^{1}H NMR (500 MHz, DMSO-*d*) δ 11.29 (s, 1H), 6.92 (s, 1H), 6.19 (t, J = 7.0 Hz, 1H), 5.21 (d, J = 4.2 Hz, 1H), 4.89 (t, J = 5.5 Hz, 1H), 4.19 (s, 1H), 4.09 (m, 2H), 3.71 (m, 1H), 3.52 (m, 2H), 2.00 (m, 2H).

5-[(*Z*)-4-(4-((Pivaloyloxy)methoxy)benzylidene)-2-methyl-5-oxo-imidazolin-1-yl]-2′-deoxyuridine (7a). 5-Amino-2′-deoxyuridine (**6**)[12] (727 mg, 3.00 mmol) and compound **3a** (949 mg, 3.00 mmol) were dissolved in dry pyridine (12 mL) and stirred at 60 °C for 22 h, then the temperature was raised to 90 °C and stirred for further 24 h. The reaction mixture was evaporated and purified by C-200 silica gel chromatography with dichloromethane–methanol (95 : 5, v/v). The eluted fraction containing the target compound was evaporated and purified again by C-200 silica gel chromatography with *n*-hexane–ethyl acetate to give compound **7a** (686 mg, 42%); ^{1}H NMR (500 MHz, DMSO-d_6) δ 11.89 (m, 1H), 8.29 (d, J = 5.1 Hz, 1H), 8.24 (d, J = 8.7 Hz, 2H), 7.15 (d, J = 8.7 Hz, 2H), 7.04 (s, 1H), 6.14 (m, 1H), 5.84 (s, 2H), 5.28 (m, 1H), 5.03 (m, 1H), 4.22 (m, 1H), 3.79 (s, 1H), 3.62–3.48 (m, 2H), 2.24–2.06 (m, 5H), 1.12 (s, 9H); ^{13}C NMR (126 MHz, DMSO-d_6) δ 176.6, 160.4, 158.0, 150.0, 141.4, 141.3, 136.9, 134.1, 128.6, 125.8, 116.3, 108.1, 87.9, 85.3, 84.9, 70.1, 70.0, 61.1, 61.1, 38.6, 26.8, 15.6, 15.5. ESI-MS calcd for $C_{26}H_{30}N_4NaO_9^+$ $[M + Na]^+$ 565.1905; found 565.1900.

5-[(*Z*)-4-(4-Hydroxybenzylidene)-2-methyl-5-oxo-imidazolin-1-yl]-2′-deoxyuridine (8a). To a solution of compound **7a** (200 mg, 0.369 mmol) in pyridine (2 mL) was added 28% aq. NH_3 (3 mL) and the reaction mixture was stirred for 7 h at room temperature. The reaction mixture was evaporated under reduced pressure. Methanol (5 mL) was added to the remaining residues and the precipitate was filtered. The residue was dissolved in water and washed with dichloromethane. The aqueous layer was collected and lyophilized to give compound **8a** (91 mg, 58%); ^{1}H NMR (500 MHz, DMSO-d_6) δ 11.83 (brs, 1H), 10.19 (brs, 1H), 8.26 (s, 1H), 8.10 (d, J = 8.6 Hz, 2H), 6.96 (s, 1H), 6.84 (d, J = 8.5 Hz, 2H), 6.19–6.08 (m, 1H), 5.30–5.21 (m, 1H), 5.02 (m, 1H), 4.23 (m, 1H), 3.78 (s, 1H), 3.61–3.47 (m, 2H), 2.25–2.05 (m, 5H); ^{13}C NMR (126 MHz, DMSO-d_6) δ 169.3, 169.2, 161.4, 161.2, 160.2, 160.0, 149.8, 149.6, 141.1, 141.0, 135.2, 134.3, 126.8, 125.1, 115.9, 108.1, 87.7, 85.1, 84.9, 70.0, 69.8, 60.9, 15.3, 15.3. ESI-MS calcd for $C_{20}H_{20}N_4NaO_7^+$ $[M + Na]^+$ 451.1224; found 451.1220.

(2,6-Difluoro-4-formylphenoxy)methyl pivalate (2b). Sodium iodide (2.09 g, 13.9 mmol) and chloromethyl pivalate (2.10 g, 13.9 mmol) were dissolved in dry acetone (25 mL) and stirred at room temperature under an argon atmosphere. After 18 h, potassium carbonate (1.93 g, 13.9 mmol) was added to the reaction mixture. Then, the reaction mixture was placed on an ice bath and 3,5-difluoro-4-hydroxybenzaldehyde (**1b**) (2.00 g, 12.7 mmol) was added. The mixture was stirred at room temperature for 27 h. After the completion of the reaction, diethyl ether was added and the precipitates were filtered. The filtrate was evaporated and purified by C-200 silica gel chromatography with *n*-hexane–ethyl acetate (96 : 4, v/v) to give compound **2b** (3.03 g, 88%); ^{1}H NMR (500 MHz, chloroform-*d*)

δ 9.85 (s, 1H), 7.46 (s, 1H), 7.45 (s, 1H), 5.76 (s, 2H), 1.16 (s, 9H); ^{13}C NMR (126 MHz, chloroform-*d*) δ 188.9, 188.7, 177.4, 157.2, 155.2, 138.8, 132.5, 113.4, 113.4, 113.3, 113.2, 88.4, 88.3, 88.0, 39.0, 26.9. ESI-MS calcd for $C_{13}H_{14}F_2NaO_4^+$ $[M + Na]^+$ 295.0752; found 295.0744.

(*Z*)-[2,6-Difluoro-4-((2-methyl-5-oxo-oxazolin-4-ylidene)methyl) phenyl]oxymethyl pivalate (3b). Compound **2b** (2.92 g, 12.4 mmol), *N*-acetylglycine (1.45 g, 12.4 mmol) and sodium acetate (1.01 g, 12.4 mmol) were dissolved in acetic anhydride (12 mL) and stirred at 100 °C for 13 h. The reaction mixture was diluted with ethyl acetate (500 mL) and washed with aq. $NaHCO_3$ and brine. The organic layer was collected, evaporated and dried over Na_2SO_4. The crude product was purified by C-200 silica gel chromatography with *n*-hexane–ethyl acetate (95 : 5, v/v) to give compound **3b** (2.47 g, 57%); ^{1}H NMR (500 MHz, chloroform-*d*) δ 7.72 (s, 1H), 7.70 (s, 1H), 6.93 (s, 1H), 5.75 (s, 2H), 2.42 (s, 3H), 1.19 (s, 9H); ^{13}C NMR (126 MHz, chloroform-*d*) δ 177.5, 167.6, 167.3, 156.9, 156.8, 154.9, 154.8, 135.7, 135.6, 135.4, 134.1, 130.0, 129.9, 129.9, 128.1, 128.1, 128.0, 115.9, 115.9, 115.8, 115.7, 88.5, 88.5, 88.5, 39.1, 27.1, 16.0. ESI-MS calcd for $C_{17}H_{17}NNaO_5^+$ $[M + Na]^+$ 376.0967; found 376.0977.

5-[(*Z*)-4-(3,5-Difluoro-2-methyl-4-((pivaloyloxy)methoxy)benzylidene)-5-oxo-imidazolin-1-yl]-2′-deoxyuridine (7b). 5-Amino-2′-deoxyuridine (**6**)[12] (688 mg, 2.83 mmol) and compound **3b** (1.0 g, 2.83 mmol) were dissolved in dry pyridine (13 mL) and stirred at 40 °C for 3 days under an argon atmosphere. The reaction mixture was evaporated and purified by C-200 silica gel chromatography with dichloromethane–methanol (97.5 : 2.5, v/v). The eluted fraction containing the target compound was evaporated and purified again by C-200 silica gel chromatography with *n*-hexane–ethyl acetate and finally eluted with ethyl acetate to give **7b** (901 mg, 55%). The analytical sample (86 mg) was obtained from the 100 mg of **7b** after recycling preparative GPC-HPLC; ^{1}H NMR (500 MHz, DMSO-d_6) δ 11.83 (s, 1H), 8.29 (s, 1H), 8.09–8.05 (m, 2H), 7.03 (s, 1H), 6.13 (m, 1H), 5.75 (m, 2H), 5.21 (s, 1H), 5.00–4.92 (m, 1H), 4.26–4.20 (m, 1H), 3.81 (d, J = 4.6 Hz, 1H), 3.64–3.49 (m, 2H), 2.23–2.10 (m, 5H), 1.12 (s, 9H); ^{13}C NMR (126 MHz, DMSO-d_6) δ 176.5, 169.0, 168.9, 165.4, 165.2, 160.1, 156.0, 156.0, 154.1, 154.0, 149.8, 141.4, 141.3, 139.2, 133.6, 131.2, 122.6, 115.6, 115.5, 115.4, 107.5, 88.2, 87.7, 85.2, 85.0, 69.9, 69.8, 60.9, 38.3, 26.6, 15.5, 15.5. ESI-MS calcd for $C_{26}H_{28}F_2N_4NaO_9^+$ $[M + Na]^+$ 601.1717; found 601.1722.

5-[(*Z*)-4-(3,5-Difluoro-4-hydroxybenzylidene)-2-methyl-5-oxo-imidazolin-1-yl]-2′-deoxyuridine (8b). To a solution of compound **7b** (67 mg, 0.116 mmol) in pyridine (0.58 mL) was added 28% aq. NH_3 (0.58 mL) and the reaction mixture was stirred for 6 h at room temperature. The reaction mixture was evaporated under reduced pressure. The crude residues were dissolved in water and a small amount of acetonitrile, and then purified by C-18 reversed phase column chromatography with water–acetonitrile (4 : 1, v/v) to give compound **8b** (22 mg, 41%); ^{1}H NMR (500 MHz, DMSO-d_6) δ 11.92–11.83 (m, 1H), 11.03 (brs, 1H) 8.27 (s, 1H), 7.97 (d, J = 9.9 Hz, 2H), 6.98 (d, J = 4.7 Hz, 1H), 6.14–6.10 (m, 1H), 5.32–5.23 (m, 1H), 5.08–4.97 (m, 1H), 4.23 (m, 1H), 3.78 (s, 1H), 3.62–3.46 (m, 2H), 2.25–2.05 (m, 5H); ^{13}C NMR (126 MHz, DMSO-d_6) δ 169.0, 163.3, 160.1, 153.0, 152.9, 151.1, 151.0, 149.7, 141.2, 141.1, 137.1, 124.3, 123.9, 115.5, 115.3, 107.7, 87.7, 85.1, 85.0, 69.9, 69.8, 60.9, 15.4, 15.4. ESI-MS calcd for $C_{20}H_{18}F_2N_4NaO_7^+$ $[M + Na]^+$ 487.1036; found 487.1028.

5′-*O*-(4,4′-Dimethoxytrityl)-5-[(*Z*)-4-(4-((pivaloyloxy)methoxy) benzylidene)-2-methyl-5-oxo-imidazolin-1-yl]-2′-deoxyuridine (9a). Compound **7a** (398 mg, 0.734 mmol) was co-evaporated with dry pyridine. Then, compound **7a** was dissolved in dry pyridine (7 mL) and 4,4′-dimethoxytrityl chloride (273 mg, 0.807 mmol) was added. The reaction mixture was stirred at room temperature for 6 h under an argon atmosphere. Then, the reaction was quenched by adding methanol (1 mL) and, the solvents were evaporated. The crude product was extracted with ethyl acetate and washed with water and then with brine. The organic layer was dried over Na_2SO_4 and evaporated. The crude product was purified by N-60 silica gel chromatography with *n*-hexane–ethyl acetate (30 : 70, v/v). The fractions containing the target compound were evaporated and again purified by N-60 silica gel chromatography with dichloromethane–methanol (96 : 4, v/v) to give compound **9a** (261 mg, 42%); ^{1}H NMR (500 MHz, DMSO-d_6) δ 11.98 (s, 1H), 8.23 (d, J = 8.2 Hz, 2H), 7.93 (s, 1H), 7.36–7.12 (m, 11H), 7.00 (m, 1H), 6.81 (m, 4H), 6.19 (t, J = 6.5 Hz, 1H), 5.85 (s, 2H), 5.37 (s, 1H), 4.34–4.22 (m, 1H), 3.91 (m, 1H), 3.68 (s, 6H), 3.32–3.03 (m, 2H), 2.27 (m, 2H), 2.07–1.98 (m, 3H), 1.12 (s, 9H); ^{13}C NMR (126 MHz, DMSO-d_6) δ 176.4, 169.2, 169.0, 162.4, 160.2, 158.0, 157.7, 149.7, 144.7, 144.6, 136.6, 135.6, 135.1, 133.9, 129.7, 129.6, 129.5, 128.4, 127.9, 127.8, 127.6, 127.6, 126.7, 125.7, 116.1, 113.2, 108.1, 85.9, 85.8, 85.6, 85.1, 84.9, 84.7, 70.5, 64.1, 63.6, 55.0, 38.4, 26.6, 15.3. ESI-MS calcd for $C_{47}H_{48}N_4NaO_{11}^+$ $[M + Na]^+$ 867.3212; found 867.3192.

5′-*O*-(4,4′-Dimethoxytrityl)-5-[(*Z*)-4-(3,5-difluoro-2-methyl-4-((pivaloyloxy)methoxy)benzylidene)-5-oxo-imidazolin-1-yl]-2′-deoxyuridine (9b). Compound **7b** (807 mg, 1.39 mmol) was co-evaporated with dry pyridine. Then, compound **7b** was dissolved in dry pyridine (14 mL) and 4,4′-dimethoxytrityl chloride (520 mg, 1.53 mmol) was added. The reaction mixture was stirred at room temperature for 7 h under an argon atmosphere. The reaction mixture was quenched by the addition of methanol and evaporated. The crude product was extracted with ethyl acetate and washed with water and then with brine. The organic layer was dried over Na_2SO_4 and evaporated. The crude product was purified by N-60 silica gel chromatography with dichloromethane–methanol (95 : 5, v/v) to give compound **9b** (770 mg, 63%); ^{1}H NMR (500 MHz, DMSO-d_6) δ 12.02 (s, 1H), 8.09 (d, J = 9.8 Hz, 2H), 7.97 (s, 1H), 7.37–7.14 (m, 9H), 7.01 (d, J = 7.5 Hz, 1H), 6.82 (m, 4H), 6.21 (t, J = 6.5 Hz, 1H), 5.75 (s, 2H), 5.39 (d, J = 4.4 Hz, 1H), 4.31 (m, 1H), 3.97–3.89 (m, 1H), 3.69 (s, 6H), 3.37–3.05 (m, 2H), 2.30 (m, 2H), 2.09 (m, 3H), 1.12 (s, 9H); ^{13}C NMR (126 MHz, DMSO-d_6) δ 176.5, 168.9, 168.8, 164.9, 164.9, 160.1, 160.0, 158.1, 158.0, 156.0, 154.1, 149.7, 144.7, 144.4, 141.1, 140.8, 139.0, 135.7, 135.4, 135.1, 133.7, 133.6, 133.4, 131.3, 131.2, 129.7, 129.4, 127.9, 127.6, 126.7, 122.7, 115.6, 115.4, 113.2, 107.8, 88.2, 86.0, 85.8, 85.7,

85.2, 84.8, 70.3, 69.9, 64.1, 63.5, 54.9, 38.3, 26.5, 15.5, 15.4. ESI-MS calcd for $C_{47}H_{46}F_2N_4NaO_{11}^+$ $[M + Na]^+$ 903.3023; found 903.3009.

5′-*O*-(4,4′-Dimethoxytrityl)-5-[(*Z*)-4-(4-((pivaloyloxy)methoxy)benzylidene)-2-methyl-5-oxo-imidazolin-1-yl]-2′-deoxyuridine 3′-(2-cyanoethyl *N*,*N*-diisopropylphosphoramidite) (10a). Compound **9a** (50 mg, 0.059 mmol) was co-evaporated with dry pyridine, dry toluene and dry dichloromethane respectively. Then, compound **9a** was dissolved in dry dichloromethane (2 mL) and diisopropylamine (5.6 μL, 0.040 mmol), 1*H*-tetrazole (2.7 mg, 0.039 mmol) and 2-cyanoethyl-*N*,*N*,*N*′,*N*′-tetraisopropylphosphordiamidite (21.4 μL, 0.067 mmol) were added respectively. The reaction mixture was stirred at room temperature for 16 h. Then, it was diluted with dichloromethane (20 mL) and washed with water, saturated aq. $NaHCO_3$, and brine. The organic layer was dried over Na_2SO_4 and evaporated. The crude product was purified by N-60 silica gel chromatography with *n*-hexane–ethyl acetate (50 : 50, v/v). The fractions containing the target compound were concentrated (22.7 mg) and directly applied for solid phase DNA synthesis.

5′-*O*-(4,4′-Dimethoxytrityl)-5-[(*Z*)-4-(3,5-difluoro-2-methyl-4-((pivaloyloxy)methoxy)benzylidene)-5-oxo-imidazolin-1-yl]-2′-deoxyuridine 3′-(2-cyanoethyl *N*,*N*-diisopropylphosphoramidite) (10b). Compound **9b** (31 mg, 0.035 mmol) was co-evaporated with dry pyridine, dry toluene and dry dichloromethane respectively. Then, compound **9b** was dissolved in dry dichloromethane (0.41 mL) and diisopropylamine (3.24 μL, 0.023 mmol), 1*H*-tetrazole (1.6 mg, 0.023 mmol) and 2-cyanoethyl-*N*,*N*,*N*′,*N*′-tetraisopropylphosphordiamidite (14.5 μL, 0.045 mmol) were added respectively. The reaction mixture was stirred at room temperature for 2.5 h, then the same amount of diisopropylamine, 1*H*-tetrazole, and 2-cyanoethyl-*N*,*N*,*N*′,*N*′-tetraisopropylphosphordiamidite was added to the reaction mixture and stirred for an additional 1.5 h to complete the reaction. Then the reaction mixture was diluted with dichloromethane (20 mL) and washed with water. The organic layer was dried over Na_2SO_4 and evaporated. The crude product was purified by N-60 silica gel chromatography with *n*-hexane–ethyl acetate (50 : 50, v/v). The fractions containing the target compound was concentrated (29.5 mg) and directly applied for solid phase DNA synthesis.

General oligodeoxynucleotide synthesis

The synthesis of oligodeoxynucleotides was carried out using an automated DNA/RNA synthesizer (ABI 392 DNA/RNA synthesizer or nS8-II) using a general protocol of ultra-mild DNA synthesis (deblocking reagent: 3% trichloroacetic acid in CH_2Cl_2, activator: 0.25 M 5-benzylthio-1*H*-tetrazole in anhydrous MeCN, capping reagents: 5% phenoxyacetic anhydride in THF–pyridine and 10% 1-methylimidazole in THF, oxidizing reagent: 0.02 M I_2 in THF–pyridine–water). The synthesis was performed on the 1 μmol scale except for **ODN-2-Y**, which was performed on the 0.2 μmol scale. The synthesized DNA was reacted with 28% aqueous ammonia solution for 12 h at ambient temperature for deprotection and cleavage from resin. The elution was evaporated under reduced pressure and then purified using a Sep-pak C18 cartridge. The DMTr group on the 5′-end was removed in the cartridge using 2% TFA in water. The DNA mixture was eluted by using 25% acetonitrile in water and then further purified by anion exchange HPLC (DNAPac PA100 9 × 250 mm) or reverse phase HPLC (XBridge C18 5 μm 4.6 × 150 mm).

Oligonucleotide synthesis containing 10a or 10b (ODN-2-Y)

DNA was firstly synthesized until **10a** or **10b** was incorporated by using the DNA/RNA synthesizer. After the synthesis, the resin was dried under reduced pressure. **10a** or **10b** (15 μmol) was co-evaporated 8 times with anhydrous acetonitrile and dissolved in anhydrous acetonitrile (150 μL) as solution A. 1*H*-Tetrazole (75 μmol, 5.25 mg) was dried under reduced pressure and then dissolved in anhydrous acetonitrile (150 μL) as solution B. Solutions A and B were added into the resin and then reacted for 45 min. After the reaction, the resin was washed with anhydrous acetonitrile and capped using 5% phenoxyacetic anhydride in THF–pyridine and 10% 1-methylimidazole in THF for 2 min. After the reaction, the resin was washed with acetonitrile and then oxidation was performed using 0.02 M I_2 in THF–pyridine–water for 1 min. The resulting resin was washed with acetonitrile, dried, and re-packed into a synthesis column for automated DNA synthesis. The rest of the synthesis was performed according to the general oligonucleotide synthesis protocol shown above except for the cleavage and deprotection conditions. Cleavage and deprotection were performed by using 28% aqueous ammonia solution for 2 h at ambient temperature for **ODN-2-Y**.

Measurements of UV and fluorescence spectra of nucleoside

The UV spectra were measured at ambient temperature using 30 μM solution of **8a** and **8b** in methanol or glycerol–methanol (95 : 5, v/v). The fluorescence spectra were measured using 100 μM solution of **8a** and 1 μM solution of **8b** prepared using the same solvents. The excited wavelengths were 380 nm for **8a** and 430 nm for **8b**.

Measurements of UV and fluorescence spectra of oligonucleotides

The oligonucleotide concentrations were determined by the standard method[18] by assuming that the molar absorption coefficients of **8a** and **8b** were identical to that of thymidine. The solutions of 2 μM of each oligodeoxynucleotide in 10 mM sodium cacodylate containing 500 mM NaCl and 10 mM $MgCl_2$ were prepared. Before the measurements, the solutions were heated at 85 °C for 5 min, and then cooled to ambient temperature. The solutions were cooled at 5 °C for 10 min and used for the measurements.

Measurements of UV-melting curves

The solutions of 2 μM of each oligodeoxynucleotide in 10 mM sodium cacodylate containing 500 mM NaCl and 10 mM $MgCl_2$ were prepared. The solutions were heated at 85 °C for 5 min, and then cooled to 5 °C. The solutions were heated

at a rate of 1 °C min^{-1}. During the melting reactions, the UV absorbances at 260 nm were monitored.

Acknowledgements

This work was supported by JSPS KAKENHI Grant Number 25810094, 25620126 and 26288075.

Notes and references

1 (*a*) M. E. Hawkins, *Cell Biochem. Biophys.*, 2001, **34**, 257; (*b*) A. Okamoto, Y. Saito and I. Saito, *J. Photochem. Photobiol., C*, 2005, **6**, 108; (*c*) J. N. Wilson and E. T. Kool, *Org. Biomol. Chem.*, 2006, **4**, 4265; (*d*) N. Venkatesan, Y. J. Seo and B. H. Kim, *Chem. Soc. Rev.*, 2008, **37**, 648; (*e*) R. W. Sinkeldam, N. J. Greco and Y. Tor, *Chem. Rev.*, 2010, **110**, 2579; (*f*) L. M. Wilhelmsson, *Q. Rev. Biophys.*, 2010, **43**, 159; (*g*) N. Dai and E. T. Kool, *Chem. Soc. Rev.*, 2011, **40**, 5756; (*h*) A. A. Tanpure, M. G. Pawar and S. G. Srivatsan, *Isr. J. Chem.*, 2013, **53**, 366.

2 (*a*) D. C. Ward, E. Reich and L. Stryer, *J. Biol. Chem.*, 1969, **244**, 1228; (*b*) A. C. Jones and R. K. Neely, *Q. Rev. Biophys.*, 2015, **48**, 244.

3 S. Lobsiger, S. Blaser, R. K. Sinha, H. M. Frey and S. Leutwyler, *Nat. Chem.*, 2014, **6**, 989.

4 J. M. Jean and K. B. Hall, *Proc. Natl. Acad. Sci. U. S. A.*, 2001, **98**, 37.

5 (*a*) O. Köhler, D. V. Jarikote and O. Seitz, *ChemBioChem*, 2005, **6**, 69; (*b*) R. W. Sinkeldam, A. J. Wheat, H. Boyaci and Y. Tor, *ChemPhysChem*, 2011, **12**, 567; (*c*) J. Riedl, P. Ménova, R. Pohl, P. Orság, M. Fojta and M. Hocek, *J. Org. Chem.*, 2012, **77**, 8287; (*d*) D. Dziuba, R. Pohl and M. Hocek, *Chem. Commun.*, 2015, **51**, 4880; (*e*) T. Kanamori, H. Ohzeki, Y. Masaki, A. Ohkubo, M. Takahashi, K. Tsuda, T. Ito, M. Shirouzu, K. Kuwasako, Y. Muto, M. Sekine and K. Seio, *ChemBioChem*, 2015, **16**, 167; (*f*) M. Tokugawa, Y. Masaki, J. C. Canggadibrata, K. Kaneko, T. Shiozawa, T. Kanamori, M. Grøtli, L. M. Wilhelmsson, M. Sekine and K. Seio, *Chem. Commun.*, 2016, **52**, 3809.

6 O. Shimomura, *FEBS Lett.*, 1979, **104**, 220.

7 (*a*) J. S. Paige, K. Y. Wu and S. R. Jaffrey, *Science*, 2011, **333**, 642; (*b*) C. L. Walker, K. A. Lukyanov, I. V. Yampolsky, A. S. Mishin, A. S. Bommarius, A. M. Duraj-Thatte, B. Azizi, L. M. Tolbert and K. M. Solntsev, *Curr. Opin. Chem. Biol.*, 2015, **27**, 64; (*c*) U. Wenge and H.-A. Wagenknecht, *Synthesis*, 2011, 502.

8 S. R. Meech, *Chem. Soc. Rev.*, 2009, **38**, 2922.

9 T. Stafforst and U. Diederichsen, *Eur. J. Org. Chem.*, 2007, 899.

10 (*a*) P. S. Patel, R. A. Shah, D. K. Trivedi and P. J. Vyas, *Orient. J. Chem.*, 2009, **25**, 111; (*b*) C.-Y. Lee, Y.-C. Chen, H.-C. Lin, Y. Jhong, C.-W. Chang, C.-H. Tsai, C.-L. Kao and T.-C. Chien, *Tetrahedron*, 2012, **68**, 5898.

11 G. Lahoud, V. Timoshchuk, A. Lebedev, K. Arar, Y. M. Hou and H. Gamper, *Nucleic Acids Res.*, 2008, **36**, 6999.

12 (*a*) M. J. Storek, A. Suciu and G. L. Verdine, *Org. Lett.*, 2002, **4**, 3867; (*b*) D. A. Barawkar, R. Krishna Kumar and K. N. Ganesh, *Tetrahedron*, 1992, **48**, 8505.

13 A. A. Voityuk, A. D. Kummer, M.-E. Michel-Beyerle and N. Rösch, *Chem. Phys.*, 2001, **269**, 83.

14 (*a*) S. A. Cassidy, P. Slickers, J. O. Trent, D. C. Capaldi, P. D. Roselt, C. B. Reese, S. Neidle and K. R. Fox, *Nucleic Acids Res.*, 1997, **25**, 4891; (*b*) M. Nakahara, Y. Hari and S. Obika, *Heterocycles*, 2012, **86**, 1135.

15 A. I. Dragan, R. Pavlovic, J. B. McGivney, J. R. Casas-Finet, E. S. Bishop, R. J. Strouse, M. A. Schenerman and C. D. Geddes, *J. Fluoresc.*, 2012, **22**, 1189.

16 (*a*) Y. Chen, S. H. Lee and C. Mao, *Angew. Chem., Int. Ed.*, 2004, **43**, 5335; (*b*) D. A. Rusling, I. S. Nandhakumar, T. Brown and K. R. Fox, *ACS Nano*, 2012, **6**, 3604; (*c*) D. A. Rusling, A. R. Chandrasekaran, Y. P. Ohayon, T. Brown, K. R. Fox, R. Sha, C. Mao and N. C. Seeman, *Angew. Chem., Int. Ed.*, 2014, **53**, 3979.

17 (*a*) T. N. Grossmann, L. Röglin and O. Seitz, *Angew. Chem., Int. Ed.*, 2007, **46**, 5223; (*b*) M. Patel, A. Dutta and H. Huang, *Anal. Bioanal. Chem.*, 2011, **400**, 3035; (*c*) J. Zheng, J. Li, Y. Jiang, J. Jin, K. Wang, R. Yang and W. Tan, *Anal. Chem.*, 2011, **83**, 6586; (*d*) F. Hövelmann and O. Seitz, *Acc. Chem. Res.*, 2016, **49**, 714.

18 P. N. Borer, *Handbook of Biochemistry and Molecular Biology*, ed. G. D. Fasman, CRC Press, Cleveland, OH, USA, 3rd edn, 1975, vol. I, p. 589.